The current data suggest that the interaction of RIM-BPs with voltage-gated Ca^{2+} channels isolates the regulation of evoked release from spontaneous fusion. However, there is growing evidence that spontaneous release events may also be regulated by voltage-gated Ca^{2+} influx, suggesting that other active zone proteins may act as the main substrate for Ca^{2+}-dependent regulation of spontaneous release (Kavalali, 2015). In sum, the study by Acuna et al. (2015) provides a new perspective on the emerging picture that single active zones not only form structural scaffolds but also function as versatile platforms that organize time-dependent properties of neurotransmitter release and render distinct forms of neurotransmitter release susceptible to selective plasticity.

REFERENCES

Acuna, C., Liu, X., Gonzalez, A., and Südhof, T.C. (2015). Neuron *87*, this issue, 1234–1247.

Eggermann, E., Bucurenciu, I., Goswami, S.P., and Jonas, P. (2012). Nat. Rev. Neurosci. *13*, 7–21.

Han, Y., Kaeser, P.S., Südhof, T.C., and Schneggenburger, R. (2011). Neuron *69*, 304–316.

Hibino, H., Pironkova, R., Onwumere, O., Vologodskaia, M., Hudspeth, A.J., and Lesage, F. (2002). Neuron *34*, 411–423.

Kaeser, P.S., Deng, L., Wang, Y., Dulubova, I., Liu, X., Rizo, J., and Südhof, T.C. (2011). Cell *144*, 282–295.

Kaeser, P.S., Deng, L., Fan, M., and Südhof, T.C. (2012). Proc. Natl. Acad. Sci. USA *109*, 11830–11835.

Kavalali, E.T. (2015). Nat. Rev. Neurosci. *16*, 5–16.

Liu, K.S., Siebert, M., Mertel, S., Knoche, E., Wegener, S., Wichmann, C., Matkovic, T., Muhammad, K., Depner, H., Mettke, C., et al. (2011). Science *334*, 1565–1569.

Mittelstaedt, T., and Schoch, S. (2007). Gene *403*, 70–79.

Müller, M., Genç, Ö., and Davis, G.W. (2015). Neuron *85*, 1056–1069.

Sabatini, B.L., and Regehr, W.G. (1996). Nature *384*, 170–172.

Schoch, S., Castillo, P.E., Jo, T., Mukherjee, K., Geppert, M., Wang, Y., Schmitz, F., Malenka, R.C., and Südhof, T.C. (2002). Nature *415*, 321–326.

Südhof, T.C. (2012). Neuron *75*, 11–25.

Vyleta, N.P., and Jonas, P. (2014). Science *343*, 665–670.

Wang, Y., Sugita, S., and Südhof, T.C. (2000). J. Biol. Chem. *275*, 20033–20044.

Superior Colliculus Does Play Dice

Daniel Kerschensteiner[1,2,3,4,*]
[1]Department of Ophthalmology and Visual Sciences
[2]Department of Anatomy and Neurobiology
[3]Department of Biomedical Engineering
[4]Hope Center for Neurological Disorders
Washington University School of Medicine, Saint Louis, MO 63110, USA
*Correspondence: dkerschensteiner@wustl.edu
http://dx.doi.org/10.1016/j.neuron.2015.09.023

Random is not a word often used in describing nervous system organization and its development. Yet, in this issue of *Neuron*, Owens et al. (2015) identify stochastic interactions of molecular and activity-dependent forces that can produce heterogeneous retinocollicular maps.

Topographic maps, in which neighboring neurons have similar functional properties (e.g., adjacent visual receptive fields), are a fundamental feature of sensory and motor systems. To produce topographic maps, nearby neurons in an input region need to connect to nearby neurons in a target region. How developing neurons establish such spatially ordered connectivity, particularly when targets are far away and intervening axons disorganized, is an intriguing question, addressed by Owens et al. (2015) for projections from the retina to superior colliculus (SC).

Retinal ganglion cell (RGC) axons innervate superficial layers of SC (Dhande et al., 2011), a midbrain structure, which integrates visual input with auditory and somatosensory information and generates commands that direct head and eye movements toward salient features of the environment (May, 2006). In the retinocollicular projection, the naso-temporal (N-T) axis of the retina is mapped onto the anterior-posterior (A-P) axis of SC, and the dorso-ventral axis of the retina is mapped onto the medio-lateral axis of SC. This superficial map of visual space is aligned with sensory and motor maps in intermediate and deep layers of SC, such that activity in motor layers directs an animal's gaze to the location represented in the overlying visual map (Schiller and Stryker, 1972).

In this issue of *Neuron*, Owens et al. (2015) examine how RGC axons achieve ordered distributions along the A-P axis of SC. This projection has long served as a model system for studies of topographic mapping (Cang and Feldheim, 2013). As part of his chemoaffinity hypothesis, Sperry proposed that "cytochemical gradients" on RGC axons and SC neurons define the positions of their connections (Sperry, 1963). Matching this prediction, EphA receptors were found to be expressed in a low-nasal to high-temporal gradient in RGCs, while SC neurons

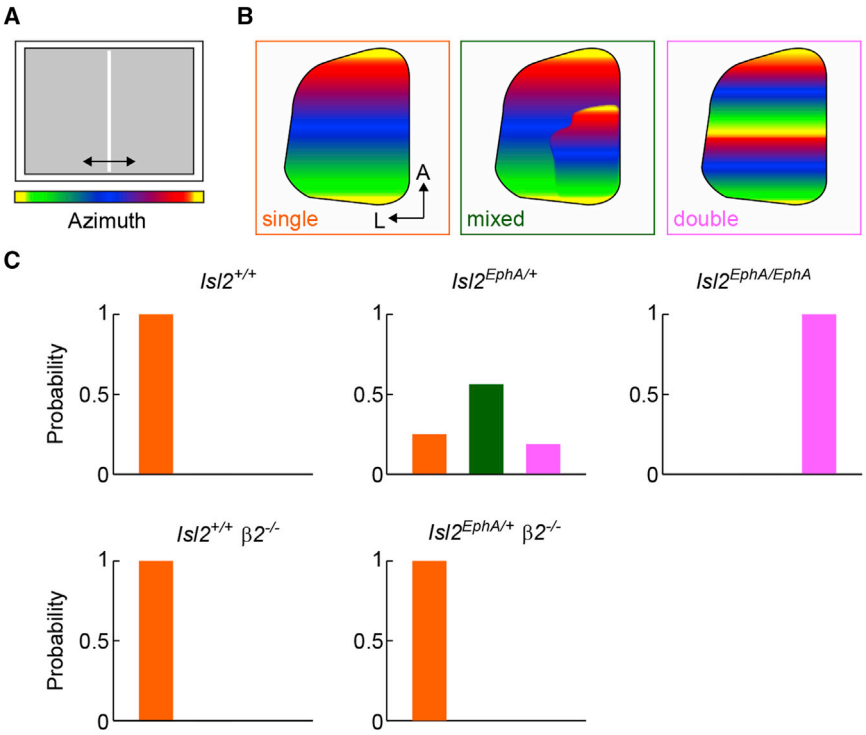

Figure 1. Visual Map Architectures and Their Distributions in Different Mouse Models
(A) Schematic of the visual stimulus presented at various azimuths.
(B) Illustration of single (left), mixed (middle), and duplicated (right) maps of visual azimuth in superior colliculus reported by Owens et al. (2015).
(C) Bar graphs summarizing the distributions of different map architectures (single, orange; mixed, green; double, pink) (B) in various mouse models. Bars in the lower left panel inferred from Mrsic-Flogel et al. (2005).

present high levels of ephrin-A ligands near the posterior and low levels near the anterior pole (McLaughlin and O'Leary, 2005). In addition, RGCs express high levels of ephrin-As in the nasal and low levels of ephrin-As in the temporal retina, whereas posterior and anterior SC neurons contain low and high levels of EphAs, respectively (McLaughlin and O'Leary, 2005). Because EphA/ephrin-A interactions mediate bidirectional repulsive signals, these opposing bilateral gradients are ideally suited to guide the mapping of RGC axons in SC. Consistent with this notion, in mice lacking EphAs or ephrin-As, RGC axons establish termination zones that are normal in structure and function but randomly positioned along the A-P axis of SC (Cang and Feldheim, 2013).

While receptor and ligand knockout mice demonstrate the importance of EphA/ephrin-A signaling, they do not reveal how gradients are used to sort RGC axons into precise maps. One critical question is whether each axon finds a unique place of least repulsion independent of other axons, or whether neighboring RGC axons compete for limited resources in SC (e.g., neurotrophic factors) based on their relative EphA/ephrin-A signaling levels. Greg Lemke's group generated mice in which these alternatives could be distinguished (Brown et al., 2000). EphA and ephrin-A families have multiple members, which interact with similar affinities in different receptor-ligand combinations (McLaughlin and O'Leary, 2005). In wild-type mice, RGCs express EphA5 and EphA6 in graded, and EphA4 in ungraded, fashion. Brown et al. (2000) inserted a cassette expressing EphA3 from and internal ribosome entry site into the *Islet2* gene. In $Isl2^{EphA/EphA}$ mice, approximately half the RGCs ($Isl2^{-}$) express EphA4, EphA5, and EphA6 as in wild-type, whereas the other half ($Isl2^{+}$) express EphA3 in addition. $Isl2^{-}$ and $Isl2^{+}$ RGCs are distributed evenly in the retina, and levels of EphA3 in $Isl2^{+}$ RGCs are constant across the retina. Anatomical tracings showed that retinocollicular maps of $Isl2^{EphA/EphA}$ mice are duplicated along the A-P axis (Brown et al., 2000). This duplication, particularly the anterior shift of axons of temporal $Isl2^{-}$ RGCs, suggests that relative rather than absolute EphA/ephrin-A signaling levels influence the position of RGC axons in SC and led to the formulation of a deterministic model of topographic mapping (Reber et al., 2004).

In this issue of *Neuron*, Owens et al. (2015) provide empirical and modeling evidence to suggest that topographic mapping of RGC axons instead emerges from a stochastic sorting process driven by relative EphA/ephrin-A signaling levels and spontaneous activity patterns. The authors use intrinsic signal imaging to analyze functional maps of visual space in SCs of wild-type (or $Isl2^{+/+}$), $Isl2^{EphA/+}$, and $Isl2^{EphA/EphA}$ mice. Consistent with previous results (Brown et al., 2000; Triplett et al., 2009), they find that representations of visual azimuth in SC are always single in wild-type and always doubled in $Isl2^{EphA/EphA}$ mice (Figure 1). By contrast, retinocollicular development of $Isl2^{EphA/+}$ mice appears to follow a probability distribution, generating single and doubled maps in about a quarter of the cases and partially duplicated (i.e., mixed) maps in the remaining half of SCs (Figure 1). Five of seven mice exhibited categorically different maps in left and right SCs, excluding variations in genetic background as a source of heterogeneity. The observation that disparate topographies can emerge from identical genetic starting points strongly suggests a stochastic mapping process.

Previous anatomical studies of $Isl2^{EphA/+}$ mice did not report heterogeneity in retinocollicular projections (Brown et al., 2000; Reber et al., 2004). To test whether the apparent discrepancy reflects differences in the sensitivity of functional and anatomical assays or may be caused by small sample sizes of previous studies, Owens et al. (2015) correlate functional imaging and anatomical tracings in a larger cohort of $Isl2^{EphA/+}$ mice. The tracing experiments reveal that axons from nasal RGCs form heterogeneous termination zones in $Isl2^{EphA/+}$ mice: the majority are split in two (similar to previous

observations), but a significant fraction are single. Importantly, single termination zones were mostly found in SCs with single functional maps, whereas split termination zones are distributed among SCs with mixed and duplicated functional maps. These results suggest that functional map heterogeneity in *Isl2*$^{EphA/+}$ mice reflects variability in the order of RGC axons in SC.

To quantitatively explore the axon sorting process, Owens et al. (2015) adapt a stochastic model of retinocollicular development (Tsigankov and Koulakov, 2010). In this model, the probability that developing RGC axons switch positions depends on the resulting changes in repulsive signaling and local activity correlations. Retinocollicular maps develop prior to vision, when the retina generates spontaneous waves of activity that spread among RGCs and propagate forward through the visual system. As waves spread across the retina they correlate the activity of RGCs in a distance-dependent manner (Kerschensteiner, 2013). Seeded with parameters that mimic conditions in wild-type and *Isl2*$^{EphA/EphA}$ mice, the stochastic model reliably generates single and duplicated topographic maps, respectively. Importantly, when parameters are adjusted to reflect lower levels of EphA3 expression in *Isl2*$^{EphA/+}$ compared to *Isl2*$^{EphA/EphA}$ mice, model runs produce heterogeneous outcomes including single, mixed, and duplicated maps. The parameter values that successfully replicate mapping phenotypes suggest that molecular and activity-dependent forces are roughly equal in strength. Owens et al. (2015) therefore explore the contribution of activity patterns to map heterogeneity experimentally. During the period of retinocollicular refinement, retinal waves are mediated by cholinergic transmission. Deletion of the β2 subunit of nicotinic acetylcholine receptors ($\beta2^{-/-}$ mice) drastically reduces the frequency of waves in vivo and alters their spatiotemporal patterns (Burbridge et al., 2014). Owens et al. (2015) find that functional maps of *Isl2*$^{EphA/+}$ $\beta2^{-/-}$ mice are uniformly single (Figure 1). Through correlation-based Hebbian plasticity mechanisms, retinal waves are thought to exert an attractive force, which drives neighboring RGCs to converge onto overlapping targets (Kerschensteiner, 2013). The observation that map coherence in SC is increased when wave frequency is reduced is thus unexpected. Given the broader spatial correlations of activity patterns in $\beta2^{-/-}$ compared to wild-type mice (Burbridge et al., 2014), it seems likely that rather than revealing hidden tendencies of waves to promote map duplication, the results of Owens et al. (2015) reflect a broadened attractive force of abnormal activity patterns, which more effectively counteracts the molecular forces driving maps toward duplication in *Isl2*$^{EphA/+}$ mice. It would be interesting, in the future, to test whether retinocollicular maps are heterogeneous in *Isl2*$^{EphA/EphA}$ $\beta2^{-/-}$ mice.

Many neural processes are stochastic, including the will-they-won't-they dynamics of vesicle fusion at axonal release sites and the trial-and-error approach of dendritic spines in search of synaptic partners. Probabilistic aspects of neural development so far were mostly thought to produce subtle differences in local wiring. The observations of Owens et al. (2015), by contrast, demonstrate the potential of stochastic processes to generate large-scale heterogeneities in nervous system organization. Given the functional disruptions that may result (e.g., from mixed or duplicated retinocollicular maps), the question arises, what is the upside of stochasticity? The answer likely involves the increased adaptive potential of networks whose organization is shaped by dynamic interactions of multiple forces (e.g., molecular gradients and activity patterns). The need for developmental plasticity may be particularly high in structures like SC that register maps of different sensory modalities and/or establish overlapping representations of different response properties in a single map. In the future, it would thus be interesting to explore whether the heterogeneity of retinotopic maps in *Isl2*$^{EphA/+}$ mice propagates to auditory, somatosensory, and motor maps deeper in SC (May, 2006), and how it affects the overlapping map of orientation selectivity recently identified in visual SC (Feinberg and Meister, 2015).

REFERENCES

Brown, A., Yates, P.A., Burrola, P., Ortuño, D., Vaidya, A., Jessell, T.M., Pfaff, S.L., O'Leary, D.D., and Lemke, G. (2000). Cell *102*, 77–88.

Burbridge, T.J., Xu, H.P., Ackman, J.B., Ge, X., Zhang, Y., Ye, M.J., Zhou, Z.J., Xu, J., Contractor, A., and Crair, M.C. (2014). Neuron *84*, 1049–1064.

Cang, J., and Feldheim, D.A. (2013). Annu. Rev. Neurosci. *36*, 51–77.

Dhande, O.S., Hua, E.W., Guh, E., Yeh, J., Bhatt, S., Zhang, Y., Ruthazer, E.S., Feller, M.B., and Crair, M.C. (2011). J. Neurosci. *31*, 3384–3399.

Feinberg, E.H., and Meister, M. (2015). Nature *519*, 229–232.

Kerschensteiner, D. (2013). Neuroscientist *20*, 272–290.

May, P.J. (2006). Prog. Brain Res. *151*, 321–378.

McLaughlin, T., and O'Leary, D.D. (2005). Annu. Rev. Neurosci. *28*, 327–355.

Mrsic-Flogel, T.D., Hofer, S.B., Creutzfeldt, C., Cloëz-Tayarani, I., Changeux, J.P., Bonhoeffer, T., and Hübener, M. (2005). J. Neurosci. *25*, 6921–6928.

Owens, M.T., Feldheim, D.A., Stryker, M.P., and Triplett, J.W. (2015). Neuron *87*, this issue, 1261–1273.

Reber, M., Burrola, P., and Lemke, G. (2004). Nature *431*, 847–853.

Schiller, P.H., and Stryker, M. (1972). J. Neurophysiol. *35*, 915–924.

Sperry, R.W. (1963). Proc. Natl. Acad. Sci. USA *50*, 703–710.

Triplett, J.W., Owens, M.T., Yamada, J., Lemke, G., Cang, J., Stryker, M.P., and Feldheim, D.A. (2009). Cell *139*, 175–185.

Tsigankov, D., and Koulakov, A.A. (2010). BMC Neurosci. *11*, 155.